High-throughput fluorescence polarization immunoassay by using a portable fluorescence polarization imaging analyzer

High-throughput fluorescence polarization immunoassay by using a portable fluorescence polarization imaging analyzer

Osamu Wakao,[a] Ken Satou,[b] Ayano Nakamura,[a] Polina Galkina,[c] Keine Nishiyama,[a] Ken Sumiyoshi,[b] Fumio Kurosawa,[d] Masatoshi Maeki,[e] Akihiko Ishida,[e] Hirofumi Tani,[e] Mikhail A. Proskurnin,[c] Koji Shigemura,[b] Akihide Hibara,[d]* and Manabu Tokeshi,[e]*

[a] Graduate School of Chemical Sciences and Engineering, Hokkaido University, Kita 13 Nishi 8, Kita-ku, Sapporo 060-8628, Japan

[b] Tianma Japan, Ltd., Shin-Kawasaki Mitsui Building West Tower 28F 1-1-2, Kashimada, Saiwai-ku, Kawasaki, Kanagawa 212-0058, Japan

[c] Chemistry Department, M. V. Lomonosov Moscow State University, Leninskie Groy, GSP-2, Moscow 119991, Russia

[d] Institute of Multidisciplinary Research for Advanced Materials, Tohoku University, Katahira 2-1-1, Aoba-ku, Sendai 980-8577, Japan

[e] Division of Applied Chemistry, Faculty of Engineering, Hokkaido University, Kita 13 Nishi 8, Kita-ku, Sapporo 060-8628, Japan

Corresponding Authors

*E-mail: hibara@tohoku.ac.jp

*E-mail: tokeshi@eng.hokudai.ac.jp

Abstract

High-throughput fluorescence polarization immunoassays (FPIAs) for mycotoxin were done using a portable FP analyzer with a microdevice. Simultaneous FPIA measurements for 8 different deoxynivalenol (DON) concentrations in 12 chambers (total of 96 samples) and high-throughput FPIA measurements for single DON concentrations in more than 500 chambers were conducted. The results indicated that simultaneous FPIAs for 96 independent samples and for 500 samples were possible by FP imaging. The FP analyzer has a size of 65 cm (W 35 cm × D 15 cm × H 15 cm) and costs less than $5000. The sample volume was 1 nL. Furthermore, it is expected that sample reaction and FP detection can be automatically conducted with the analyzer by changing the microdevice and the software. Its features such as the low cost and portability will contribute to on-site measurement and point-of-care testing. Additionally, the high-throughput feature will contribute to the study of molecular interactions based on FP measurements.

Introduction

Fluorescence polarization immunoassay (FPIA) is one of the well-established homogeneous competitive immunoassays for quantification of target analyte.   Since FPIA has a short measurement time and it is easy to implement, it is widely used in food analysis, clinical and biomedical applications.[1-15]   In FPIA measurements, P, namely the degree of polarization, is determined using the following equation:

$$P = (I_\parallel - I_\perp) / (I_\parallel + I_\perp) \tag{1}$$

where $I_\parallel$ and $I_\perp$ are fluorescence intensities with parallel and perpendicular polarizations to the excitation polarization, respectively.   FPIA is based on the competitive binding reaction between target analyte and fluorescent labeled target analyte (tracer) to an antibody.[1]   In FPIA, the amount of tracer molecules and antibody molecules are fixed as constant.   When the analyte molecule concentration is low, most of the tracer molecules bind to the antibody so that P becomes high.   On the other hand, when the analyte concentration is high, most of the analyte molecules bind to the antibody so that free tracer molecules are still present and P becomes low.   The required process for the measurements is mixing of analyte, tracer and antibody solutions.   Therefore, FPIA does not require antibody immobilizations and washing steps that lead to handling complexity and a long measurement time as in heterogeneous immunoassays.   Because of its convenience, FPIA is applied to quantitative analysis of residual drugs[2,3] and mycotoxins[4,5] in food, therapeutic drugs in body fluids,[6,7] and so on.

In FPIA measurements, to measure P, fluorescence has to be separately measured as parallel polarization ($I_\parallel$) and perpendicular polarization ($I_\perp$).   In the conventional FP measurement systems, a pair of polarizers,[8,9] a rotating polarizer,[10,11] or a polarizing beam splitter[12,13] is usually used for the polarization separation.   These measurement mechanisms are limited to a single analysis so that the measurement throughput is low.   Although commercial fluorescence microplate readers provide high-throughput FP measurements, these readers adopt an optical scanning method, which requires additional complex optical components that make the measurement system large and expensive.[14,15]   In addition, the sample volume for the measurements is large so that whole measurement cost becomes high.

Previously, we proposed a FP measurement principle using a liquid crystal (LC) layer and an image sensor, which enables simultaneous multi-sample FPIA by FP imaging.[16,17]   The FP measurement principle was based on

3

the synchronized detection between the modulation frequency of FP that was transmitted through the LC layer and the image sampling frequency of the image sensor.   Implementation of this principle realized imaging of P for multiple samples in a single measurement.   Based on this principle, we developed a FP measurement system with an inexpensive LED and suitable high-transmittance LC layer.[18]   The developed system could conduct simultaneous FPIA measurements of multiple samples, and the measurement precision of the system was comparable with that of the conventional FP apparatus designed for single sample analysis.   In addition, we anticipated that the system had potential for further downsizing, cost reduction, and throughput increase.

In this paper, we developed a portable FP analyzer with a microdevice which realized high-throughput FPIA measurements.   The portable FP measurement analyzer was developed by changing its optical form and components in order to downsize and reduce the cost.   An inexpensive complementary metal-oxide semiconductor (CMOS) sensor was used as a detector instead of a CCD camera, and the optical arrangement was designed for downsizing.   A personal computer (PC) and digital analog converter (DAC), which controls the FP imaging with our homebuilt software, were packaged with all the optics.   First, to confirm the measurement performance, we conducted simultaneous FPIAs of 96 mycotoxin samples using a suitably designed microdevice with the FP analyzer. Additionally, to prove the potential for high-throughput analysis, we conducted FPIAs for more than 500 samples. The results indicated that high-throughput FPIA measurements for mycotoxin were achieved.   The FP analyzer cost less than \$5000 and had a size of 65 cm (W 35 cm × D 15 cm × H 15 cm) and the measurement sample volume was three million times lower (1 nL) than that of the conventional method (3 mL).

Experimental

Fluorescence polarization measurement principle

The measurement principle was based on the synchronized detection between the LC orientation frequency and the CMOS image sampling frequency.   The LC layer modulates the FP, which is emitted from the sample and transmitted through the LC layer, at a certain frequency (f Hz) by applied voltage of the LC layer.   When such a modulated FP is detected by the CMOS sensor at four times larger frequency ($4f$ Hz) than the modulated frequency,

four images with FP are sampled.   By image processing using these four images, an amplitude component (AC)

image and a direct component (DC) image are acquired as:

$$AC = \frac{\sqrt{2}T}{2\pi}(I_\parallel - I_\perp) \qquad\qquad (2)$$

$$DC = \frac{T}{8}(I_\parallel + I_\perp) \qquad\qquad (3)$$

where T is the period.   Luminance of the AC image includes different components of FP and luminance of DC

image includes summed components of FP.   Thus, P value is obtained as a single two-dimensional image, namely

the P image, by modifying these equations as:

$$P = \frac{I_\parallel - I_\perp}{I_\parallel + I_\perp} = \frac{\pi\ AC}{4\sqrt{2}DC}. \qquad\qquad (4)$$

Thus, if multiple samples in the visual field of the CMOS sensor are captured as a single P image, it is possible to

simultaneously obtain the P values of all the samples by reading out the luminance value of each sample part in the

P image.

Portable FP analyzer

A conceptual illustration of the optical setup for the portable FP analyzer with a CMOS sensor is shown in Fig. 1.

In order to collimate the excitation beam which was emitted from a 470 nm wavelength LED an aspheric condenser

lens was used (L1 in the figure).   The excitation beam was focused on the blades of an iris diaphragm by using

plano-convex lens (L2).   In order to make the beam profile uniform, the iris diaphragm removed the unnecessary

part of the beam.   The excitation beam was collimated again by a condenser lens (L3).   In order to make the

overall size of the analyzer compact, the collimated beam was reflected by a prism mirror.   After passing through

a linear glass polarizing filter, the polarized excitation beam entered a dichroic block with an excitation filter and a

dichroic mirror.   The dichroic mirror reflected the excitation beam, and then the beam was also reflected by a prism

mirror to reduce the overall size of the analyzer.   The excitation beam was focused onto a microdevice, which held

the sample to be imaged, by a objective lens (L4).   The sample had an emission wavelength of approximately 520

nm.   The fluorescence was collected by the aspheric lens and passed through the dichroic mirror and the emission

filter.   A high-transmittance LC layer (MS-β14A, Tianma Japan, Kawasaki, Japan) with a polarizing filter

modulated the polarization of the fluorescence which passed through the LC layer.   By passing through another

imaging lens (L5), the fluorescence focused on a CMOS image sensor, and then the polarization of the fluorescence

was captured as AC or DC images.   In order to produce P images, the captured images were processed using

homebuilt software implemented by a board personal computer (PC).   The homebuilt software was designed using

Microsoft Visual Studio to adjust the CMOS sensor control.   The frequency of the high-transmittance LC layer

orientation and that of image sampling for the CMOS sensor were synchronized using a digital analog converter

(DAC) with a ratio of 1:4.   The voltage applied to the high-transmittance LC layer was manually designed to fit

the measurement conditions (60 Hz; < 8 V).   The analyzer included the optical setup, PC, and DAC in its housing,

and schematic illustration and a photo of it with a smartphone (iPhone 7, Apple Inc., CA, USA) are shown in Figs.

2(A) and 2(B), respectively.   The FP analyzer cost less than $5000 and had a size of 65 cm (W 35 cm × D 15 cm

× H 15 cm) which made it portable.

Fig 3 shows schematic illustration of FPIA measurement procedure.   First, target, fluorescein-conjugated

target and antibody are mixed and the mixture is introduced into a microdevice.   Second, the images of the

microdevice are captured and processed to produce P images according to the formula[16] using home-built image

processing software.   Then, the FP values of sample are detected by reading out the luminance of the P image.

Chemicals

The commercial fluorescence polarization immunoassay kit (Aokin Mycontrol DON) for deoxynivalenol (DON)

measurement was purchased from Aokin AG (Berlin, Germany).   The kit contained control DON, fluorescein-

conjugated DON, anti-DON antibodies, and buffer for dilution.   The tracer had an excitation wavelength of 470

nm and emission wavelength of 520 nm.   The sample preparation was performed according to the instructions of

the kit manufacturer.   DON standard was diluted as 8 different concentrations (2.4, 4.8, 9.6, 19.2, 38.5, 76.9, 153.8,

and 615.4 ng/mL) and then mixed with fluorescein-conjugated DON and anti-DON antibodies.   From there, the

sample filled the microchambers, and excess sample in the microchannel was removed by air injection from the

inlet. In this paper, we demonstrated simultaneous multi-sample FPIAs for DON using the developed portable

analyzer to evaluate its performance.   FP measurements on a similar sample were also performed using a

commercial conventional FP apparatus (FP-715, JASCO Co., Tokyo, Japan) and a commercial microplate reader (Infinite 200 PRO, Tecan Group Ltd., Männedorf, Switzerland) to compare their performance. The Sylgard 184 Silicone Elastomer Kit for polydimethylsiloxane (PDMS) microdevice fabrication was purchased from Dow Corning Toray Co., Ltd. (Tokyo, Japan). The PDMS included black silicon rubber to decrease the background. Negative photoresist (SU-8 3050) for PDMS microdevice fabrication was purchased from Nippon Kayaku Co., Ltd. (Tokyo, Japan).

Fabrication of PDMS-glass microdevice

The PDMS-glass microdevice was fabricated using the standard soft lithography technique.[19] Negative photoresist SU-8 3050 was spin-coated onto a silicon wafer (Sumco Co., Tokyo, Japan) at 1300 rpm. The spin-coated wafer was baked at 95 °C for 45 min on a hot plate. After the baking, the wafer was exposed to UV light which was passed through a photomask designed by a mask aligner (M-1S, Mikasa Co., Ltd., Tokyo, Japan) to fabricate a mold. The mold was coated with trichloro(1H, 1H, 2H, 2H-perfluorooctyl) silane. PDMS prepolymer (Sylgard 184) was mixed with black silicon rubber- to an OD value of 10 using a mixer (ARE-310, Thinky Co., Tokyo, Japan). PDMS prepolymer with black silicon rubber was then mixed with a crosslinking curing agent at a weight ratio of 10:1. The PDMS prepolymer with black silicon rubber and the curing agent was cast on the mold and cured at 80 °C for 60 min. After peeling the cured PDMS off the mold, the PDMS, which the microdevice design had been transferred to, was pasted on a glass slide. Figs. 4(A) and 4(B) show photos of the typical clear PDMS microdevice and the black PDMS microdevice which included black silicon rubber, respectively.

First, simultaneous FPIAs of 96 mycotoxin samples were conducted. In this experiment, the microdevice had eight microchannels, each with an individual inlet and outlet, and could hold eight different samples. Each microchannel had twelve microchambers so that realized 96 samples measurement. Figs. 5(A) and 5(B) are a schematic illustration of the design and a fluorescence image of the 96 samples, respectively. Each microchannel was 100 μm wide and 100 μm deep with 12 microchambers. Each microchamber was a cube with side lengths of 100 μm and each sample volume was 1 nL. Air was removed from the microdevice by applying adequate vacuum; then the sample was dropped into the inlet and introduced into the microchannel by suction from the outlet.[20] From

there, the sample filled the microchambers, and excess sample in the microchannel was removed by air injection from the inlet.   The microdevice was able to obtain measurements for 96 samples in the same field of view. Second, high-throughput FPIAs for more than 500 samples were conducted to prove the potential for high-throughput analysis.   In this experiment, the PDMS had 625 microchambers that were cubes with side lengths of 100 μm.   By interposing the sample between the PDMS and the glass, the sample filled with the microdevice.   Fig. 6 shows a fluorescence image of 625 independent samples.   The excitation beam of the analyzer was irradiated as a circular shape, so the microdevice was able to obtain about 500 samples in the same field of view.

Results and discussion

Simultaneous FPIA measurements of different mycotoxin concentrations

Here, we demonstrated simultaneous multi-sample FPIAs for DON using the developed portable analyzer that realized FP imaging to evaluate the analyzer performance.   DON is produced by one of the fungal pathogens of grains, namely *Fusarium graminearum*, which causes a disease known as Fusarium head blight[21].   DON has been found in grains such as wheat, corn, rye, rice, and barley worldwide[22].   Because of its toxicity, the Codex Alimentarius Commission has determined a maximum reference value of 2 mg/kg in grains for processing.   FPIA has been employed as a rapid and simple method to detect DON concentrations; however, FPIA throughput is low[23,24] and another alternative, microplate readers, require optical scanning.[25]

First, the simultaneous FPIA measurements of 8 different DON concentrations (2.4, 4.8, 9.6, 19.2, 38.5, 76.9, 153.8, and 615.4 ng/mL) in 12 chambers (total of 96 samples) were conducted.   The mixture of DON, fluorescein-conjugated DON, and anti-DON antibodies was incubated and then introduced into the microchambers.   Fig. 7 shows typical AC, DC, and *P* images of the DON samples.   The luminance of the *P* image that reflected the *P* values was gradually changed by the FP values of each sample.   The *P* value measured by the portable analyzer was determined by reading out the luminance of the area of a microchamber on the *P* image.   Fig. 8 shows sets of standard curves of the *P* values against DON concentrations (from 2.4 ng/mL to 615.4 ng/mL) obtained by the portable FP analyzer and the conventional apparatus (FP-715).   The measurements were performed in triplicate, so each plotted point of the portable FP analyzer represented the total results from 288 microchambers.   As

8

expected, the relaxation of FP from the 288 microchambers was observed with increasing DON concentration, which is typical for FPIA.   Results from both the developed analyzer and the conventional analyzer were correlated, thereby indicating that simultaneous FPIAs for 96 independent samples were possible with the analyzer.   A conventional microplate reader also realized measurements of the 96 samples; however, the reader requires sample scanning which necessitates inclusion of additional complex optical components.   On the other hand, the FP analyzer developed here realized FP imaging for all 96 samples as a single two-dimensional image, so scanning was not necessary.

High-throughput FPIA measurements for mycotoxin

Second, we conducted the simultaneous FPIA measurements of single DON concentrations (2.4, 4.8, 9.6, 19.2, 38.5, 76.9, 153.8, and 615.4 ng/mL) in more than 500 chambers.   The microdevices were filled with the sample by interposing the sample between the PDMS and the glass.   Fig.9 shows typical AC, DC, and P images of the DON samples.   Fig.10 shows sets of standard curves of P values against DON concentrations (from 2.4 ng/mL to 615.4 ng/mL) obtained by the portable FP analyzer and the conventional apparatus (FP-715).   The measurements were performed in triplicate, so each plotted point of the portable FP analyzer represents the total results from 1500-1539 microchambers.   Results from both the developed analyzer and the conventional analyzer were correlated, thereby indicating that simultaneous FPIA for more than 500 independent samples was possible with the portable FP analyzer.

We realized high-throughput FPIA for mycotoxin.   The larger error bars of the results obtained with the analyzer than those of the results obtained with the conventional FP apparatus were attributed to the heterogeneity of polarization in the field of view.   When the high-throughput FPIA was conducted, measured FP values from each area of the microchambers disagreed because of the analyzer characteristics.   The heterogeneity of polarization was attributed to the optics (mainly the dichroic mirror), LC layer, and CMOS sensor; however, we expect that it is possible to correct for this using software in the near future.   Additionally, the detection accuracy is still low because the number of pixels for detection was only 100.   Through further optimization of the optics (lenses and filters), microdevice design (dimensions), area of the measurement detection (the number of pixels), and

9

detection conditions (CMOS exposure time and the number of sampling images), among others, improvement in the detection accuracy is possible.

The results showed the portable FP analyzer feature high-throughput.   The number of samples can be adjusted for the applications by changing the microdevice design.   Additionally, the mixer structure is easily integrated into the microdevice, so mixing for FPIA reactions can also be conducted on the analyzer.   As a trial experiment, the mixing of DON sample solution containing tracer with antibody solution was conducted on the microdevice, and then, the mixture was directly measured by the FP analyzer (see the Electronic supplementary information for details).   From results of FPIA measurements for 3 different DON concentrations (2.4, 19.2, and 153.8 ng/mL), the relaxation of FP was observed with increasing DON concentration.   These results showed that the FP analyzer had a great potential for further high-throughput FPIA by integrating the mixing steps for the FPIA reactions.   Therefore, it will be possible to realize totally automatic high-throughput FPIA in the near future.

Conclusions

We conducted high-throughput FPIAs for mycotoxin using a portable FP analyzer.   First, simultaneous FPIA measurements for 8 different DON concentrations in 12 chambers (total of 96 samples) were conducted.   The results indicated that simultaneous FPIAs for 96 independent samples were possible by FP imaging without any scanning process.   Second, high-throughput FPIA measurements for single DON concentrations in more than 500 chambers were conducted.   The number of samples could be adjusted according to the application, and a mixing process could be conducted on the FP analyzer by changing the microdevice design.   Therefore, we expected that totally automatic high-throughput FPIA was possible by integrating the mixing steps for analytes, tracers, and antibodies.

Table 1 compares the specifications and capabilities of the FP analyzer, the conventional commercial apparatus (FP-715), and the microplate-based apparatus (Infinite 200 PRO).   The present analyzer had many advantages compared with the others.   The FP analyzer has a size of 65 cm (W 35 cm × D 15 cm × H 15 cm) and costs less than $5000; furthermore, the FP analyzer has the potential for further downsizing and price reduction by optimizing the optical components and electronics.   The measurement sample volume was three million times

lower (1 nL) than that of the conventional apparatus (3 mL).   As well, sample reaction and FP detection can be automatically conducted with the analyzer by changing the microdevice and the software.   In the current system, the smaller the chamber size, the worse the measurement accuracy.   This is due to in-plane non-uniformity of the degree of polarization, which can be improved by optimizing the optics and improving the measurement software. Features such as the low cost and portability of the FP analyzer will contribute to on-site measurement and point-of-care testing.   In particular, the on-site measurements for mycotoxins are valuable for easily checking grain growth.   Additionally, the high-throughput feature of the analyzer will contribute to the study of molecular interactions.   The measurement throughput of the portable FP analyzer still remains low because the measurement time has not been optimized.   The measurement time has the potential to be much better through optimization of the exposure time, frequencies, and microdevice design.   Some studies on molecular interactions, such as protein-protein, protein-DNA, and protein-ligand binding interactions, have employed FP measurements because of their simplicity.[26-28]   The FP analyzer will be able to conduct high-throughput sample reactions and FP detections automatically, so only sample injections will need to be done by researchers.   Therefore, the portable FP analyzer with high-throughput has the potential to contribute to researchers in various fields and to the safety of foods for consumers.
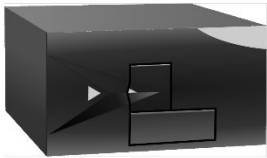
Electronic supplementary information

Supplementary material related to this article can be found in XXX

References

1. D. S. Smith and S. A. Eremin, *Anal. Bioanal. Chem.*, 2008, **391**, 1499-1507

2. C. Li, Y. Zhang, S. A. Eremin, O. Yakup, G. Yao and X. Zhang, *Food Chem.*, 2017, **227**, 48-54

3. Z. Wang, S. Zhang, N. R. Murtazina, S. A. Eremin and J. Shen, *IJFST,* 2008, **43**, 114-122

4. C. Maragos, *Toxins*, 2009, **1**, 196-207

5. M. S. Nasir and M. E. Jolley, *J. Agric. Food Chem.*, 2002, **50**, 3116-3121

6. T. Tachi, T. Hase, Y. Okamoto, N. Kaji, T. Arima, H. Matsumoto, M. Kondo, M. Tokeshi, Y. Hasegawa and Y. Baba, *Anal. Bioanal. Chem.*, 2011, **401**, 2301-2305

7. B. Glahn-Martínez, E. Benito-Peña, F. Salis, A. B. Descalzo, G. Orellana and M. C. Moreno-Bond, *Anal. Chem.*, 2018, **90**, 5459-5465

8. D. M. Jameson and J. A. Ross, *Chem. Rev.*, 2010, **110**, 2685-2708

9. L. F. Cheow, R. Viswanatha, C.-S. Chin, N. Jennifer, R. C. Jones, E. Guccione, S. R. Quake and W. F. Burkholder, *Anal. Chem.*, 2014, **86**, 9901-9908

10. T. Tachi, N. Kaji, M. Tokeshi and Y. Baba, *Lab. Chip.*, 2009, **9**, 966-971

11. Z. Zhou, X. Yan, Y. Lai and R. N. Zare, *J. Phys. Chem. Lett.*, 2018, **9**, 2928-2932

12. J. Choi, D. Kang, H. Park, A. J. deMello and S. Chang, *Anal. Chem.*, 2012, **84**, 3849-3854

13. Z. Zhao, L. Wei, M. Cao and M. Lu, *Biosens. Bioelectron.*, 2019, **128**, 91-96

14. J. Inglese, C. E. Shamu and R. K. Guy, *Nat. Chem. Biol.*, 2007, **3**, 438-441

15. A. Minas, A. Stournara, M. Minas, J. Stack, E. Petridou, G. Christodoulopoulos and V. Krikelis, *J. Immunol. Methods*, 2007, **320**, 94-103

16. O. Wakao, Y. Fujii, M. Maeki, A. Ishida, H. Tani, A. Hibara and M. Tokeshi, *Anal. Chem.*, 2015, **87**, 9647-9652

17. O. Wakao, M. Maeki, A. Ishida, H. Tani, A. Hibara and M. Tokeshi, *Sens. Actuator B*, 2019, **285**, 418-422

18. O. Wakao, K. Satou, A. Nakamura, K. Sumiyoshi, M. Shirokawa, C. Mizokuchi, K. Shiota, M. Maeki, A. Ishida, H. Tani, K. Shigemura, A. Hibara and M. Tokeshi, *Rev. Sci. Instrum.*, 2018, **89**, 024103

19. N. Kimura, M. Maeki, Y. Sato, Y. Note, A. Ishida, H. Tani, H. Harashima and M. Tokeshi, *ACS Omega.*, 2018, **3**, 5044-5051

20. K. Nishiyama, K. Sugiura, N. Kaji, M. Tokeshi and Y. Baba, *Lab. Chip.*, 2019, **19**, 233-240

21. C. M. Maragos and R. D. Platter, *J. Agric. Food Chem.*, 2002, **50**, 1827-1832

22. C.M. Placinta, J. P. F. D'Mello and A. M. C. Macdonald, *Anim. Feed Sci. Technol.*, 1999, **78**, 21-37

23. M. Z. Zheng, J. L. Richard and J. Binder, *Mycopathologia*, 2006, **161**, 261-273

24. M. S. Nasir and M. E. Jolley, *Comb. Chem. High Throughput Screen.*, 2003, **6**, 267-273

25. C. Li, K. Wen, T. Mi, X. Zhang, H. Zhang, S. Zhang, J. Shen, and Z. Wang, *Biosens. Bioelectron.*, 2016, **79**, 258-265

26. B. Wang, D. Ren, Z. You, Y. Yalikun and Y. Tanaka, *Analyst*, 2018, **148**, 3560-3569

27. M. M. Makowski, C. Gräwe, B. M. Foster, N. V. Nguyen, T. Bartke and M. Vermeulen, *Nat. Commun.*, 2018, **9**, 1653

28. J. R. Lundblad, M. Laurance and R. H. Goodman, *Mol. Endocrinol.*, 1996, **10**, 607-612

Table 1 Comparison of the specifications and capabilities of the developed portable FP analyzer, conventional commercial apparatus, and microplate-based apparatus.

System	Developed FP analyzer	Conventional apparatus	Microplate reader
Appearance			
Size (W×H×D mm^3) Weight	350×150×100, 5.5 kg	297×220×420, ~20 kg	425×253×457, 14 kg
Polarizer	LC	Filter	Filter
Detector	CMOS	PMT	PMT
Number of samples	>500 at a time	1	96
Measurement throughput*	5.0 samples/s	0.5 samples/s	4.8 samples/s
Sample volume	1 nL	> 2 mL	200 µL
Precision**	<11.0% for 1 sample < 24.5% for 500 samples	< 8.1%	< 6.6%
Cost	<$5,000	~$10,000	~$30,000
Portability	✓	×	×
Mix	✓***	×	✓

*The measurement throughput was calculated from the ratio of the number of samples at a time to the measurement time.

**The precision was calculated from the ratio of error bars to the dynamic range of DON measurement. For single sample detection, the precision (< 11%) was almost the same as that of the conventional apparatus.

***The mixing process can be integrated into the analyzer by changing the microdevice design (see the Electronic supplementary information for details).

Figure Captions

Fig. 1 Concept illustration of the optical setup for the portable FP analyzer with a CMOS sensor (L, lens; PF, polarizing filter; ExF, excitation filter; D, dichroic mirror; M, mirror; S, sample; and EmF, emission filter).

Fig. 2 (A) Schematic illustration of the portable FP analyzer which includes the optical setup with a PC and DAC in its housing.   (B) Photo of the portable FP analyzer with a smartphone (iPhone 7).   The FP analyzer cost less than $5000 and had a size of 65 cm (W 35 cm × D 15 cm × H 15 cm) making it portable.

Fig. 3 Schematic illustration of FPIA measurement procedure.

Fig. 4 Photos of the (A) clear PDMS microdevice and the (B) black PDMS microdevice which included black silicon rubber with a five yen coin (5 JPN, 22 mm in diameter).

Fig. 5 Microdevice for measurement of 96 samples.   (A) Schematic illustration of the design and (B) a fluorescence image of the 1 mM fluorescein remaining in the 96 microchambers.   Each microchannel was 100 μm wide and 100 μm deep with 12 microchambers.   Each microchamber was a cube with side lengths of 100 μm so that each sample volume was 1 nL.   The microdevice could obtain measurements for 96 samples in the same field of view of the FP analyzer.

Fig. 6 Fluorescence image of 625 independent samples.   The microchambers were filled with 1 mM fluorescein. Each microchamber was a cube with side lengths of 100 μm so that each sample volume was 1 nL.   Spacing between the microchannels was 50 μm.   The microdevice could obtain measurements for more than 500 samples in the same field of view of the FP analyzer.

Fig. 7 Typical images obtained by the FP analyzer for the DON FPIA.   (A) AC image, (B) DC image, and (C) *P* image of eight different DON concentration samples.   Each sample filled 12 microchambers.   The scale bars are 500 μm.

Fig. 8 Standard curves of FP against DON concentrations obtained using the portable FP analyzer and a conventional apparatus that was designed for a single sample analysis.   The measurements were performed in triplicate, so each plotted value of the portable FP analyzer represents the total results from 288 microchambers.

Fig.9 Typical images obtained by the FP analyzer for the DON FPIA.   (A) AC image, (B) DC image, and (C) *P* image of > 500 microchambers filled with single DON concentration samples.   The scale bars are 500 μm.

Fig.10 Standard curves of FP against DON concentrations obtained by the portable FP analyzer and the conventional apparatus that was designed for single sample analysis.   The number of microchambers for each measurement was 500-520.   The measurements were performed in triplicate, so each plotted value of the portable FP analyzer represents the total results from 1500-1539 microchambers.

Fig.1

(A)

(B)

Fig.2

Fig. 3

(A)

(B)

Fig. 4

(A)

45 mm

18 mm

100 µm

100 µm

100 µm

(B)

500 µm

Fig.5

Fig.6

(A)

(B)
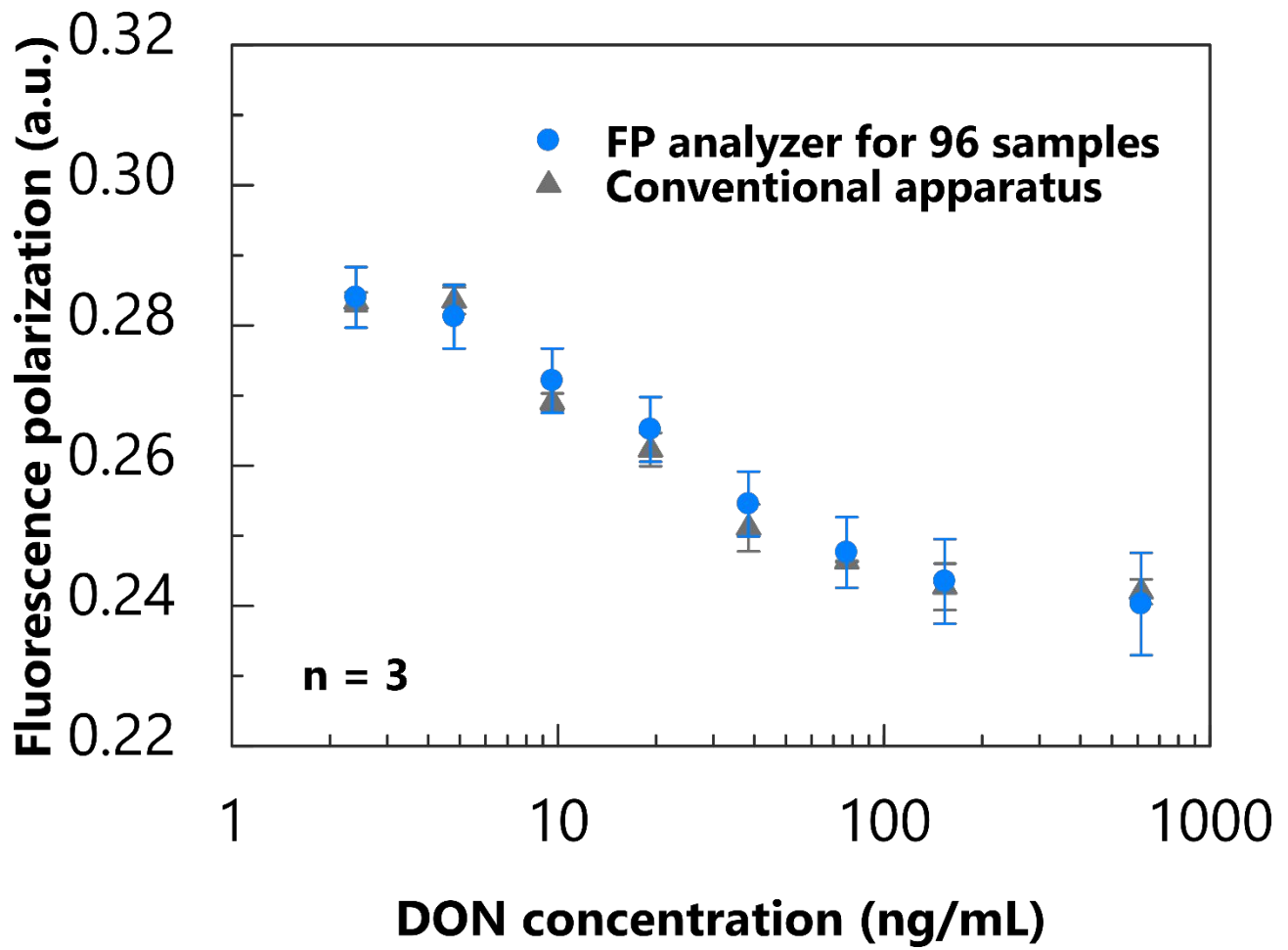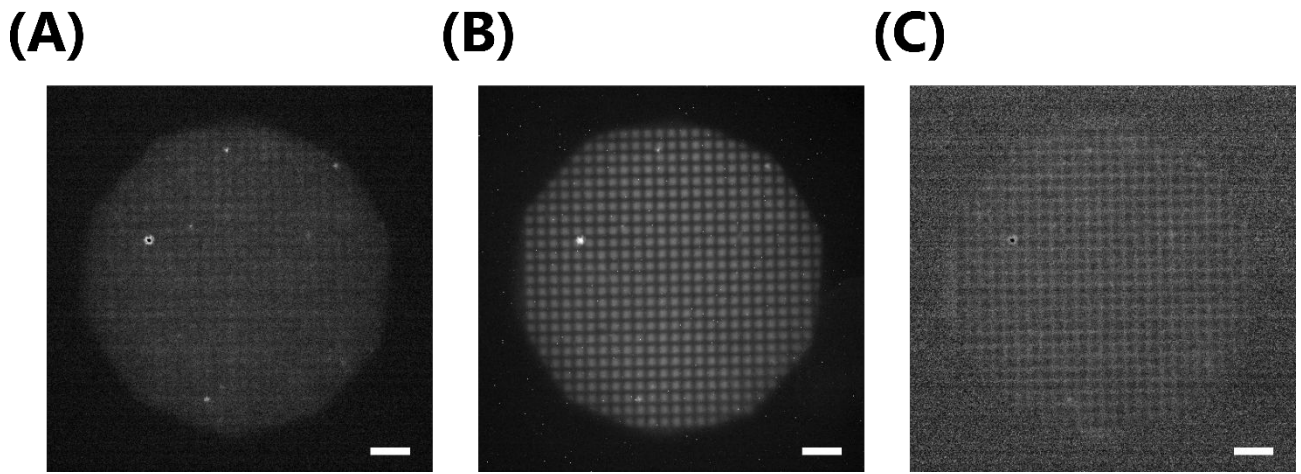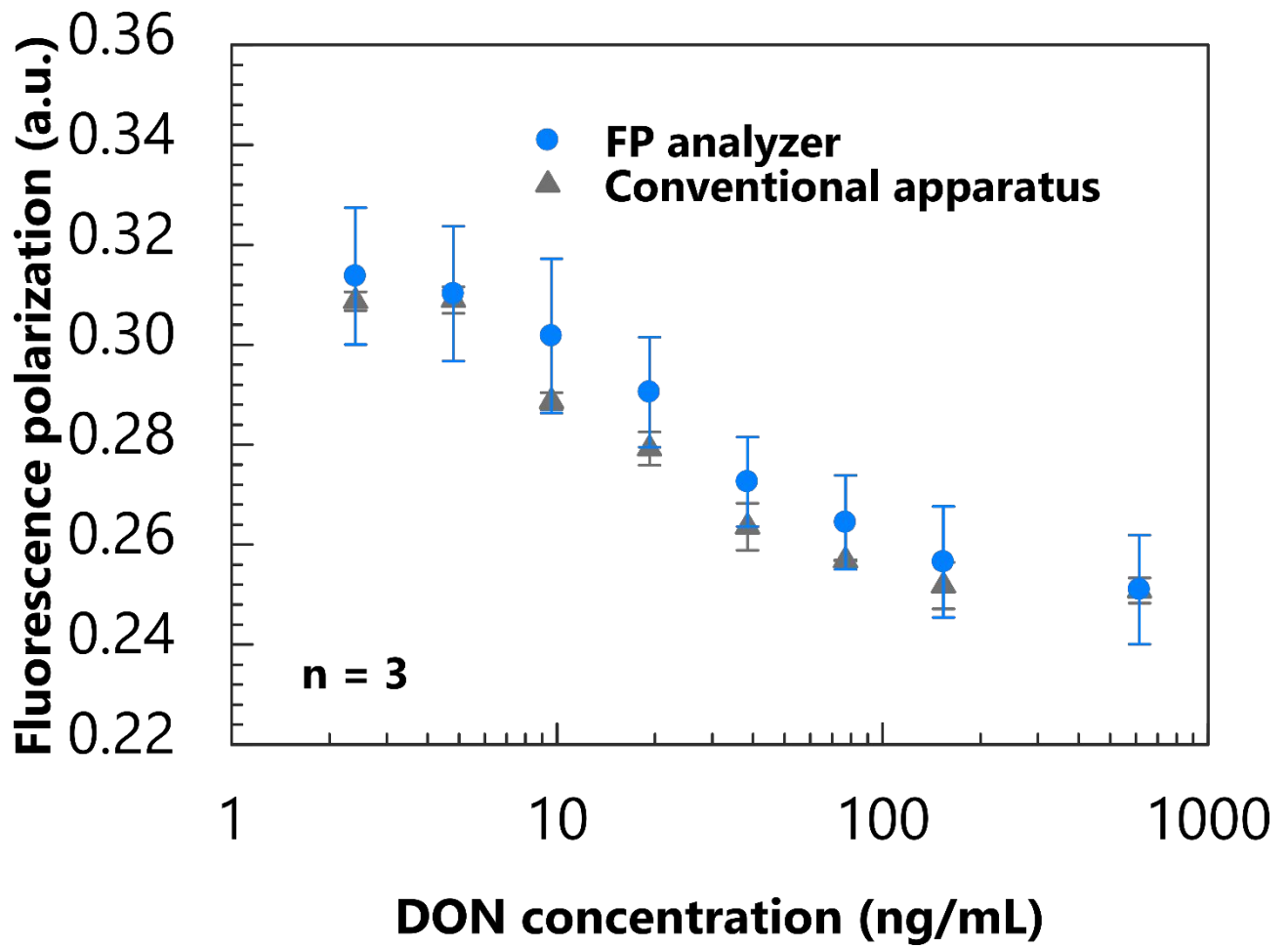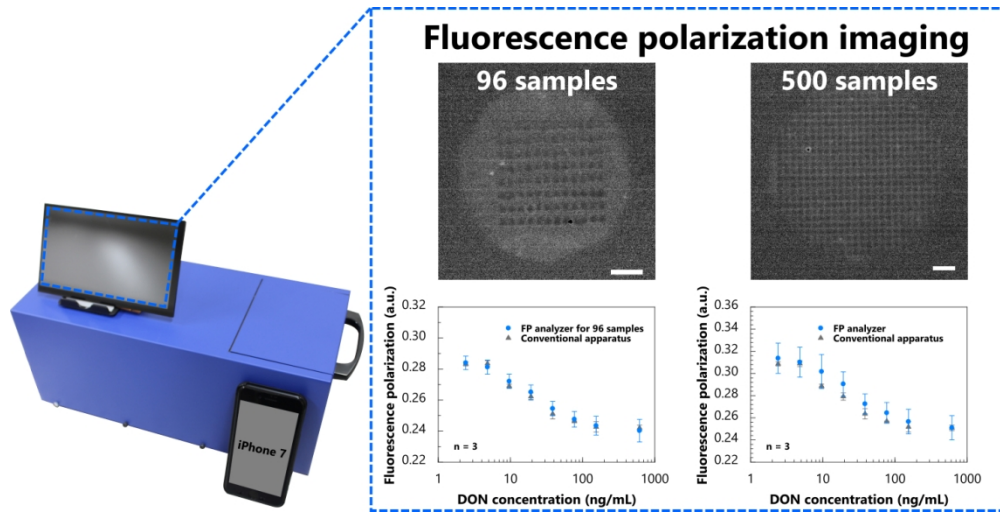
(C)

Fig.7

Fig.8

(A)   **(B)**   **(C)**
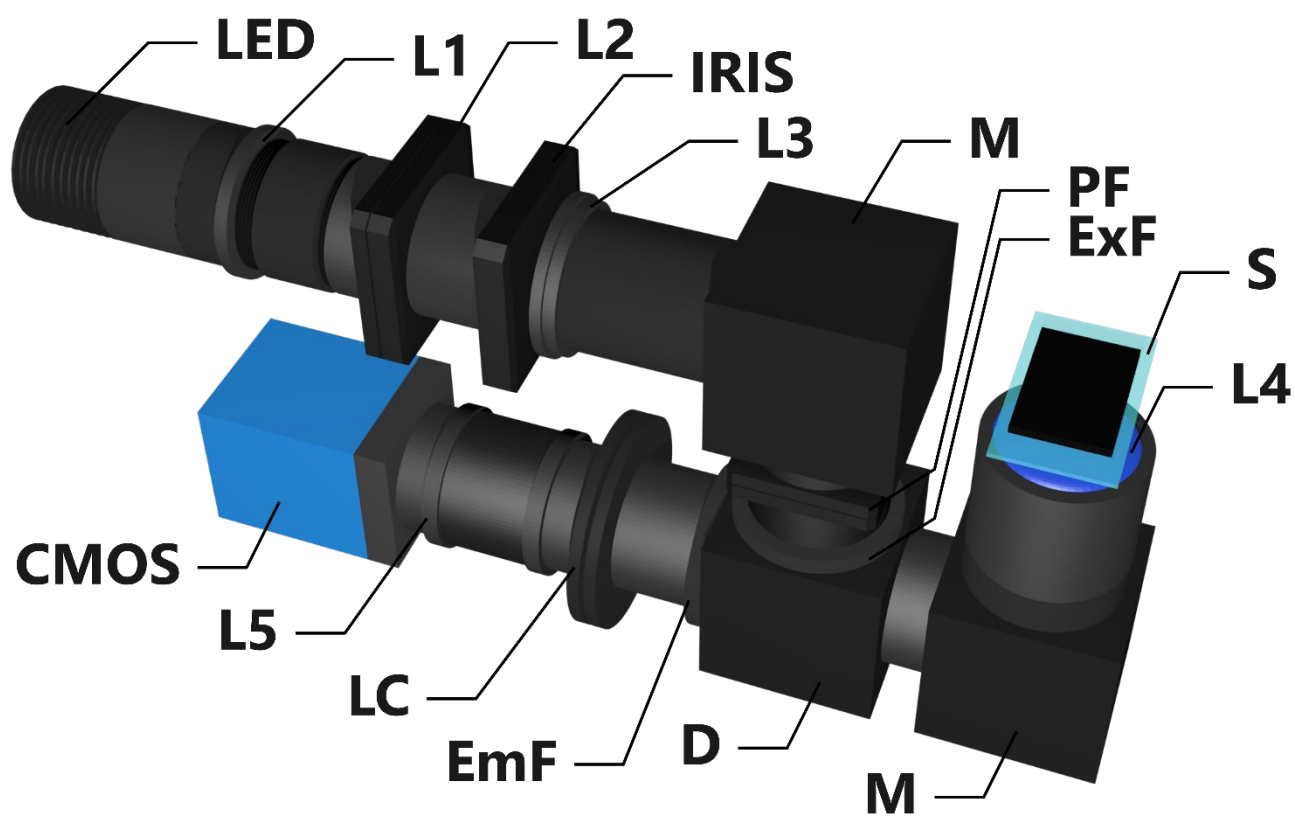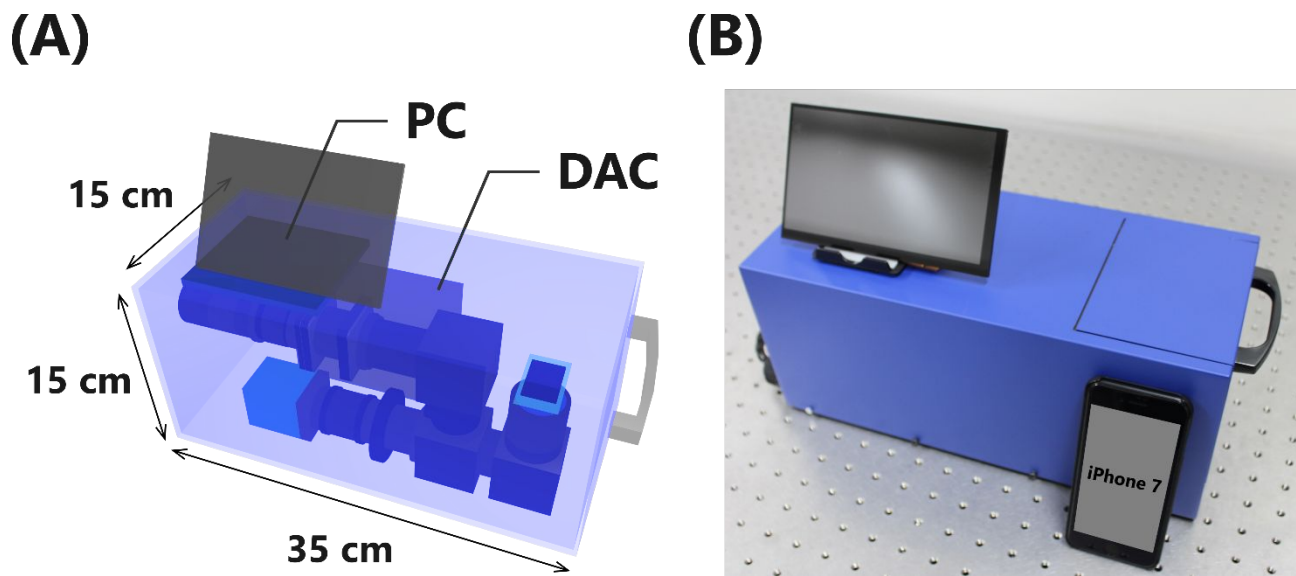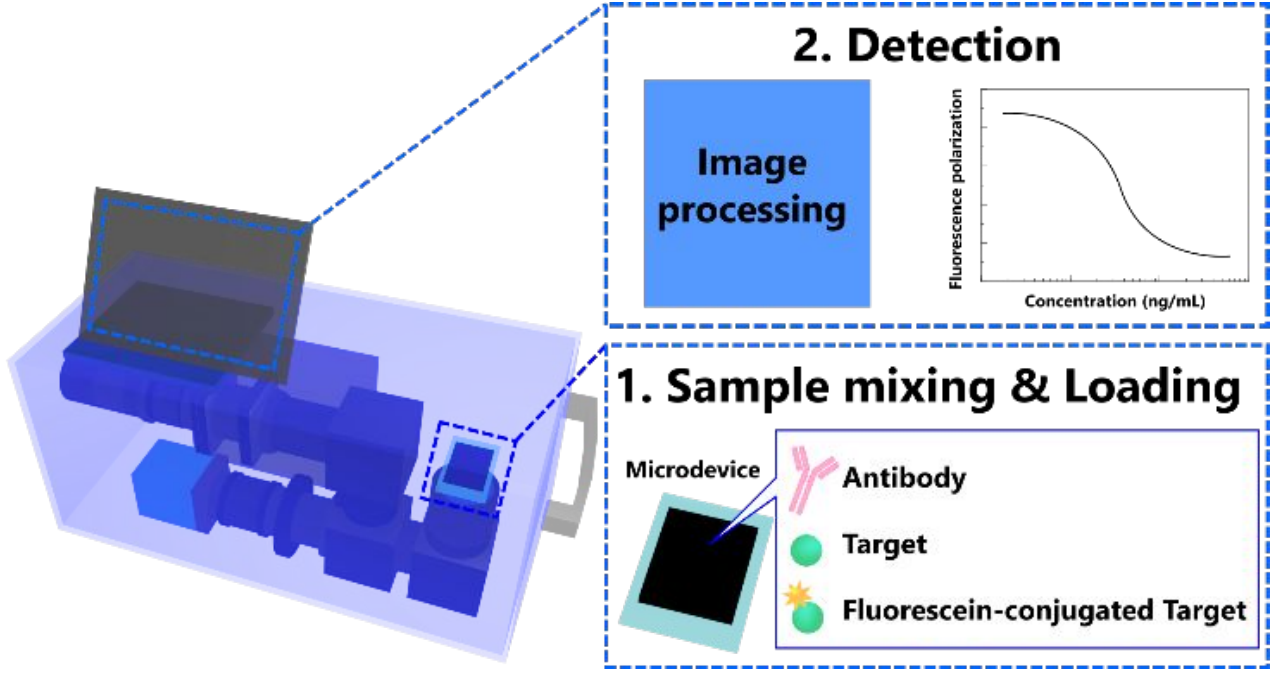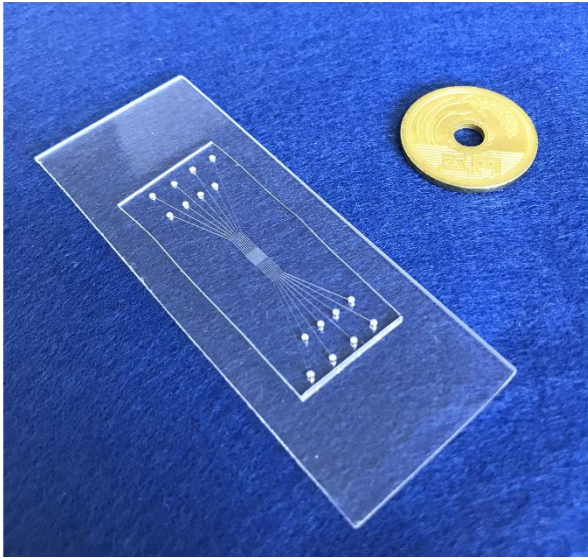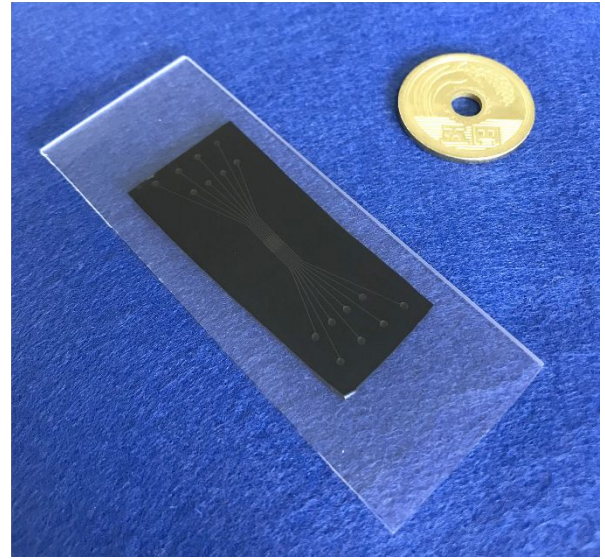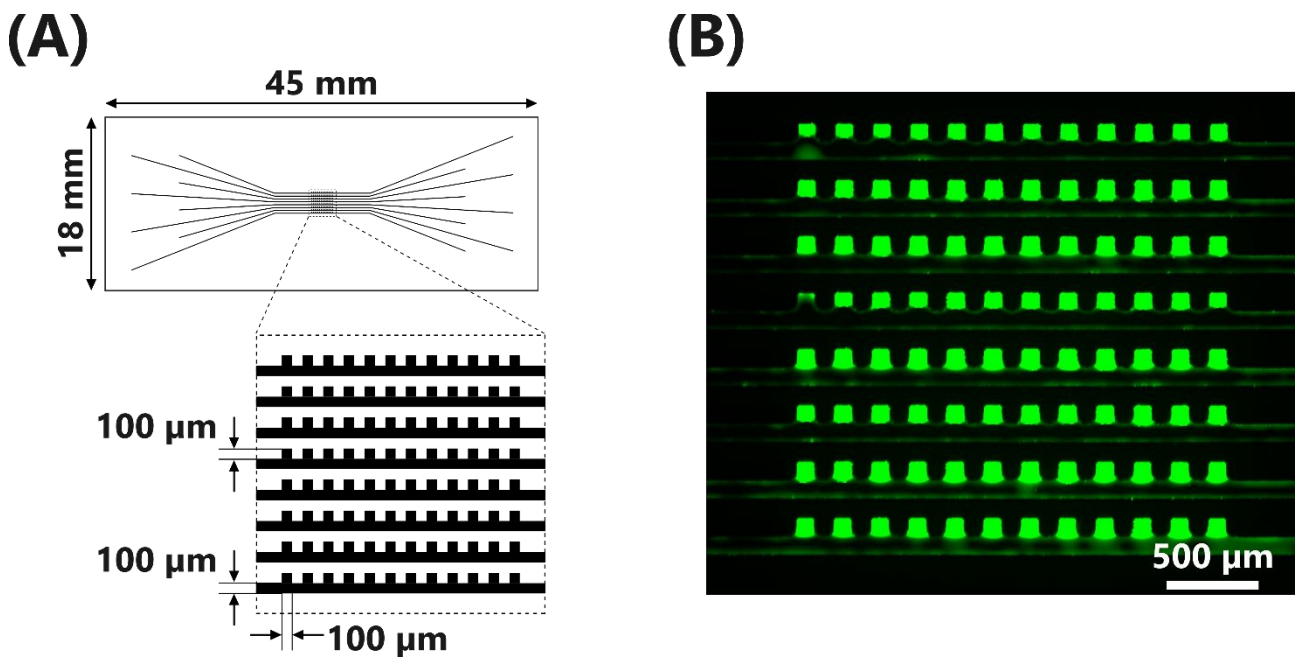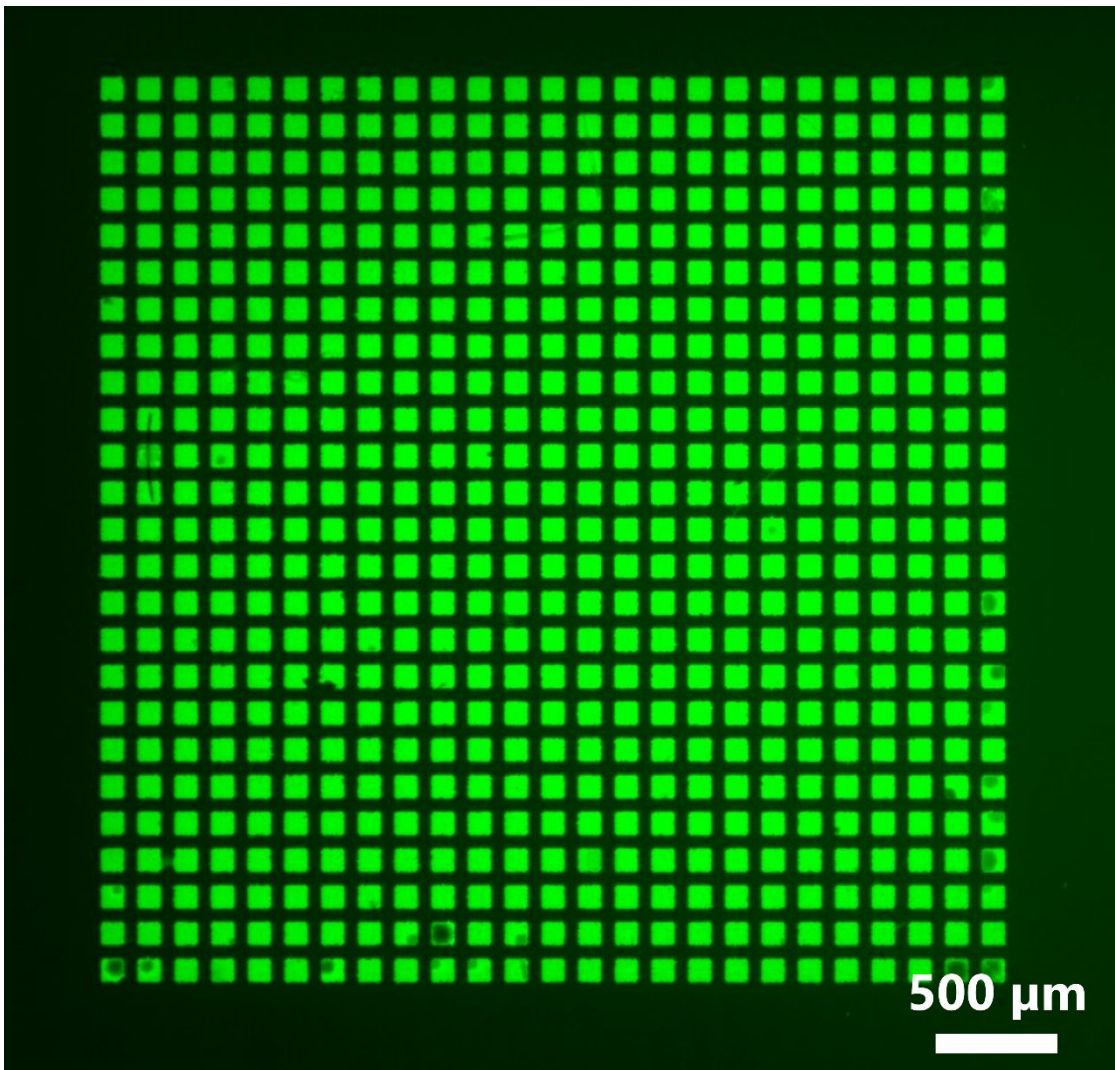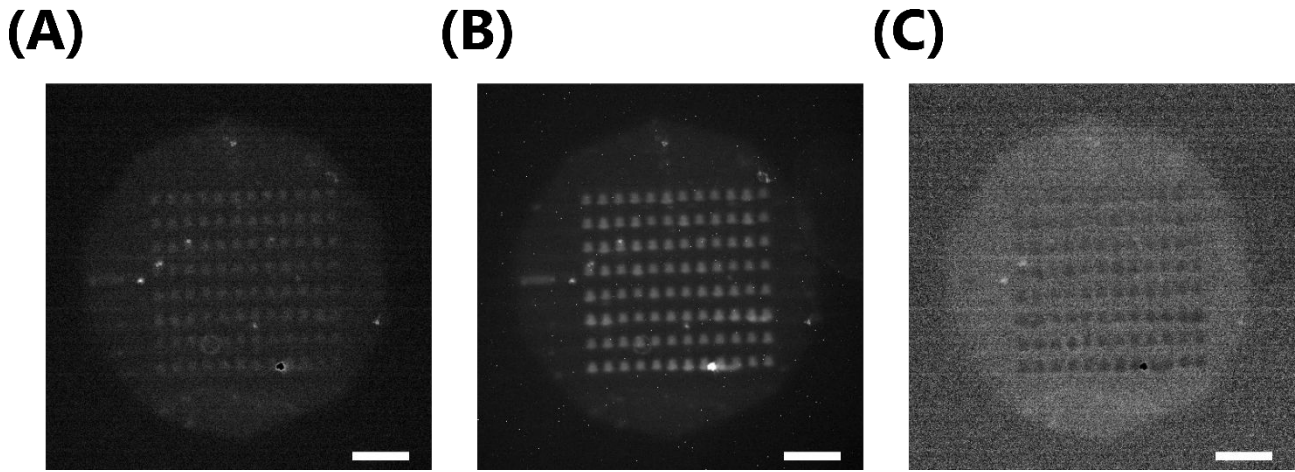
Fig.9

Fig.10

for Abstract

521x263mm (72 x 72 DPI)